



## Enhanced adsorption of norfloxacin on modified TiO<sub>2</sub> particles prepared via surface molecular imprinting technique

Song Li, Lei Fang\*, Miaomiao Ye, Yan Zhang

*Institute of Municipal Engineering, Zhejiang University, Hangzhou 310058, P.R. China, Tel. +86 571 88206759; email: lisong\_001@hotmail.com (S. Li), Tel. +86 571 88206759; Fax: +86 571 88208721; email: fanglei1999@126.com (L. Fang), Tel. +86 571 88206759; emails: yemiao008@zju.edu.cn (M. Ye), zhangyan@zju.edu.cn (Y. Zhang)*

Received 9 November 2014; Accepted 2 March 2015

### ABSTRACT

For norfloxacin removal in aquatic environment, TiO<sub>2</sub> particles (P25) were modified via surface molecular imprinting technique to improve the adsorption property and sustainable use by photocatalytic regeneration. Orthogonal experiment was adopted to quantify the significance of preparation factors and determine the optimum preparation conditions. The adsorption of norfloxacin on the molecular imprinted particles (MIPs), the non-imprinted particles (NIPs), and P25 fitted the second-order adsorption model and Langmuir model well. The MIPs showed a higher adsorption capacity toward norfloxacin than the NIPs and P25. The adsorption rate constant, maximum adsorption capacity, and Langmuir constant of the MIPs toward norfloxacin were 0.49 g mg<sup>-1</sup> min<sup>-1</sup>, 2.99 mg g<sup>-1</sup>, and 2.4 L mg<sup>-1</sup>, respectively. Removal efficiencies for norfloxacin, ciprofloxacin, carbamazepine, and phenol by the MIPs were 76.99, 78.81, 7.87, and 2.68%, respectively, which indicated that the MIPs had higher affinity toward norfloxacin and fluoroquinolones with similar structures. Moreover, the MIPs exhibited the photocatalytic property and could be regenerated by UV irradiation with stable removal efficiency for norfloxacin in five adsorption–regeneration cycles.

*Keywords:* Surface molecular imprinting technique; Adsorption; Photocatalytic regeneration; Norfloxacin

### 1. Introduction

Fluoroquinolones, which have been widely used in human and veterinary medicine because of their high antibacterial activity against both gram-negative and gram-positive bacteria through inhibition of DNA gyrase, are one of the most important synthetic antibiotics worldwide [1]. Previous works [2,3] have found that, only less than a quarter of fluoroquinolones can be metabolized in the body and most of them are

excreted largely unchanged and eventually discharged into the environment. It has been proved that the trace fluoroquinolones in wastewater and surface water can lead to the resistance of the bacteria to antibiotic and thus, pose a potential threat to the environment and human health [4]. However, the traditional water treatment technology cannot sufficiently or efficiently remove all fluoroquinolones [5–7]. Hence, developing more effective and practical methods to remove such trace organic contaminants from water is of great interest.

\*Corresponding author.

Norfloxacin is one of the mostly common used fluoroquinolones in the urinary tract infections treatment [8]. It has been detected frequently in wastewater and surface water at levels ranging from  $\text{ng L}^{-1}$  up to  $\text{mg L}^{-1}$  [9]. Because of its antibacterial property, norfloxacin can hardly be removed by biodegradation process [10]. Hitherto many novel methods have been developed for the removal of norfloxacin. Haque and Muneer [2] and Li et al. [11] have studied the performance of norfloxacin degradation by photocatalysis. Rivas et al. [12] have employed the method in combination of ozone and ultraviolet radiation to degrade norfloxacin in aqueous solutions. Liu et al. [6] have prepared the lotus stalk-based activated carbon and iron-doped activated alumina to remove norfloxacin by adsorption. Yang et al. [13] studied the adsorption behavior and mechanisms of norfloxacin onto porous resins and carbon nanotube. However, most of these methods have no selectivity toward norfloxacin and thus may not effectively remove norfloxacin with low concentration under the coexistence of other organic matters with high concentration. Therefore, the molecular imprinting technique, which can improve the selectivity of adsorbents, was adopted in our work to prepare the adsorbents for norfloxacin.

Previous works have proved that molecular imprinting is a useful technique to construct specific sites for the target compounds and the molecular imprinted polymers display the enhanced selective adsorption ability [14]. Researchers have tried to prepare molecular imprinted materials for the extraction of target substances [15,16] and selective removal of trace pollutants such as carbamazepine [17], perfluorooctane sulfonate [18], arsenic [19], and estrogenic compounds [20,21] from aqueous solutions. The results have showed that the molecular imprinted adsorbents have favorable adsorption performance and selective recognition ability. For the preparation of inorganic molecular imprinted modified  $\text{TiO}_2$ , liquid-phase deposition method [22,23] and one-step sol-gel method [24] have been developed. The inorganic molecular imprinted modified  $\text{TiO}_2$  showed higher stability than the materials prepared using organic materials as functional monomers and crosslinker. Based on the previous works about the inorganic molecular imprinted modified  $\text{TiO}_2$  material, some interesting aspects need to be further investigated. Firstly, the previous studies mainly focused on their photocatalytic performance. The adsorption performance, adsorption mechanism, and selective recognition ability were of interest for further research. Secondly, during the elution of template molecules and the regeneration process of the adsorbents, the eluent and eluate might also become the pollutants, so

that the preparation method should be improved. Thirdly, the factors that influence the preparation of the molecular imprinted adsorbents were investigated individually and the interaction between these factors did not take into consideration in the previous works.

The objectives of our study were to prepare molecular imprinted materials with both selective adsorption and photocatalytic regeneration ability for sustainable removal of norfloxacin in aquatic environment. In our work, the  $\text{TiO}_2$  nanoparticles (P25) were used as the support and crystallization reagent, which contribute to the growing of the imprinting layers on the nanoparticles [25]. The MIPs were prepared by liquid-phase deposition method, and the preparation conditions were optimized by orthogonal experiment analysis. The MIPs prepared under the optimized condition were characterized. The adsorption kinetics, isotherms, and thermodynamic were studied and the results were compared between the MIPs, the non-imprinted particles (NIPs), and P25 in order to investigate their adsorption performance and mechanism in detail. The removal efficiencies of the adsorbents toward norfloxacin, ciprofloxacin, carbamazepine, and phenol were tested to verify the selectivity of the MIPs toward certain molecules. UV irradiation, which was a moderate regeneration method, was adopted to regenerate the MIPs and the regeneration performance was also evaluated through five adsorption–regeneration cycles.

## 2. Materials and methods

### 2.1. Chemicals and materials

Norfloxacin and ciprofloxacin with a purity of  $\geq 98\%$  were purchased from Aladdin Industrial Inc. (China), while carbamazepine and phenol with a purity of  $\geq 99\%$  were supplied by Sigma-Aldrich (USA). Acetonitrile and phosphoric acid, which were of HPLC grade, were also purchased from Sigma-Aldrich (USA). Ammonium hexafluorotitanate and boric acid were of analytical grade and were obtained from Sino-pharm Chemical Regent Co., Ltd. (China).  $\text{TiO}_2$  particles (P25) were provided by Degussa (Germany). Ultrapure water was used for the preparation of all aqueous solutions. The 300 W UV lamp was purchased from Nanjing Xujiang electromechanical plant (China).

### 2.2. Preparation and characterization of the MIPs

The MIPs were prepared by an improved liquid-phase deposition method. Firstly, norfloxacin was dissolved in ultrapure water to form a solution at a

concentration of 200 mg L<sup>-1</sup>. Ammonium hexafluorotitanate and boric acid were then sequentially added under stirring at the concentration of 0.02 and 0.04 mol L<sup>-1</sup>, respectively. After they had been all dissolved, P25 was added at a concentration of 2 g L<sup>-1</sup>. The prepared solution was kept in a water bath at 30°C with stirring for 2 h and deposited at the same temperature for 2 h. The solid particles were separated from the suspension by centrifuge. The obtained materials were dried to constant weight and then calcined at 350°C in muffle furnace for 3 h. The NIPs were prepared by the same procedures without norfloxacin in the deposition solution. The preparation condition had been optimized by orthogonal experiments. The adsorption performance of the MIPs prepared under different conditions was tested with the initial aqueous norfloxacin concentration of 1 mg L<sup>-1</sup> and the results were analyzed. The optimal preparation condition was then obtained.

The morphological characterization of the samples was carried out using a transmission electron microscope (JEM-1230, JEOL Ltd, Japan) and scanning electron microscope (XL30-ESEMFEI, Philips, the Netherlands). X-ray diffraction analysis was carried out by X'Pert PRO X-ray diffractometer (PANalytical B.V., the Netherlands) to determine the crystalline structure of the samples. The surface areas and the pore parameters of the samples were also measured and analyzed by TriStar II 3020 surface area and porosity analyzer (Micromeritics Instrument Corporation, USA).

### 2.3. Adsorption performance

Batch adsorption experiments were carried out at 25°C and 250 rpm on the orbital shaker (KS 4000 i control, IKA, Germany) using flasks containing norfloxacin solution with an initial concentration of 1 mg L<sup>-1</sup> and a certain amount of the MIPs with stopper. For adsorption kinetics experiment, the specimens were sampled at defined time intervals from 10 to 100 min. The adsorption isotherms were investigated over various initial concentrations ranging from 0.1 to 10 mg L<sup>-1</sup>. Adsorption thermodynamics experiments were conducted at 15, 20, 25, 30, and 35°C. Adsorption performance of the MIPs, NIPs, and P25 toward ciprofloxacin, carbamazepine, and phenol was also evaluated under the initial concentration of 1 mg L<sup>-1</sup>, respectively, in order to indicate the selectivity of the adsorbents. The removal efficiency was defined as:

$$E = \frac{c_1 - c_2}{c_1} \quad (1)$$

where  $c_1$  and  $c_2$  (mg/L) were the initial and equilibrium adsorbates' concentrations, respectively.

### 2.4. Regeneration experiments

The regeneration of the MIPs was investigated through five adsorption–regeneration cycles. The saturated MIPs were irradiated under 300 W UV lamp with stirring for 2 h to degrade the adsorbed norfloxacin, and then the adsorption sites of the MIPs were recovered. The regenerated MIPs were reused in the next cycle of adsorption experiments. Each adsorption process last 4 h, which had been proved to reach the adsorption equilibrium within this period in preliminary experiment.

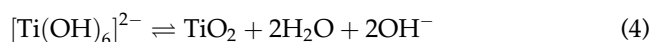
### 2.5. Analytical methods

After the adsorption experiments, the solutions were filtrated by the filter with 0.22 μm membranes. The concentrations of the norfloxacin, ciprofloxacin, carbamazepine, and phenol were determined using an Agilent 1200 series HPLC (Agilent Technologies, USA) with FLD and UV detector. The XDB-C18 column (4.6 × 150 mm) from Agilent Technologies was applied with a flow rate of 1.0 mL min<sup>-1</sup> at 25°C. The mobile phase was acetonitrile/0.1% phosphoric acid solution (30/70, v/v). The excitation and emission wavelength used in the FLD detector for determination of norfloxacin and ciprofloxacin was 280 and 450 nm, respectively. For the determination of phenol, the value was set to 275 and 313 nm, respectively. UV detector was set at 284 nm to detect carbamazepine. The injection volume was programmed at 10 μL.

## 3. Results and discussion

### 3.1. Optimization of MIPs preparation

The liquid-phase deposition method was used to prepare the MIPs adsorbents in our work. The preparation procedure was shown in Fig. 1. The mechanism for the preparation of the MIPs could be expressed as Eqs. (2)–(4).



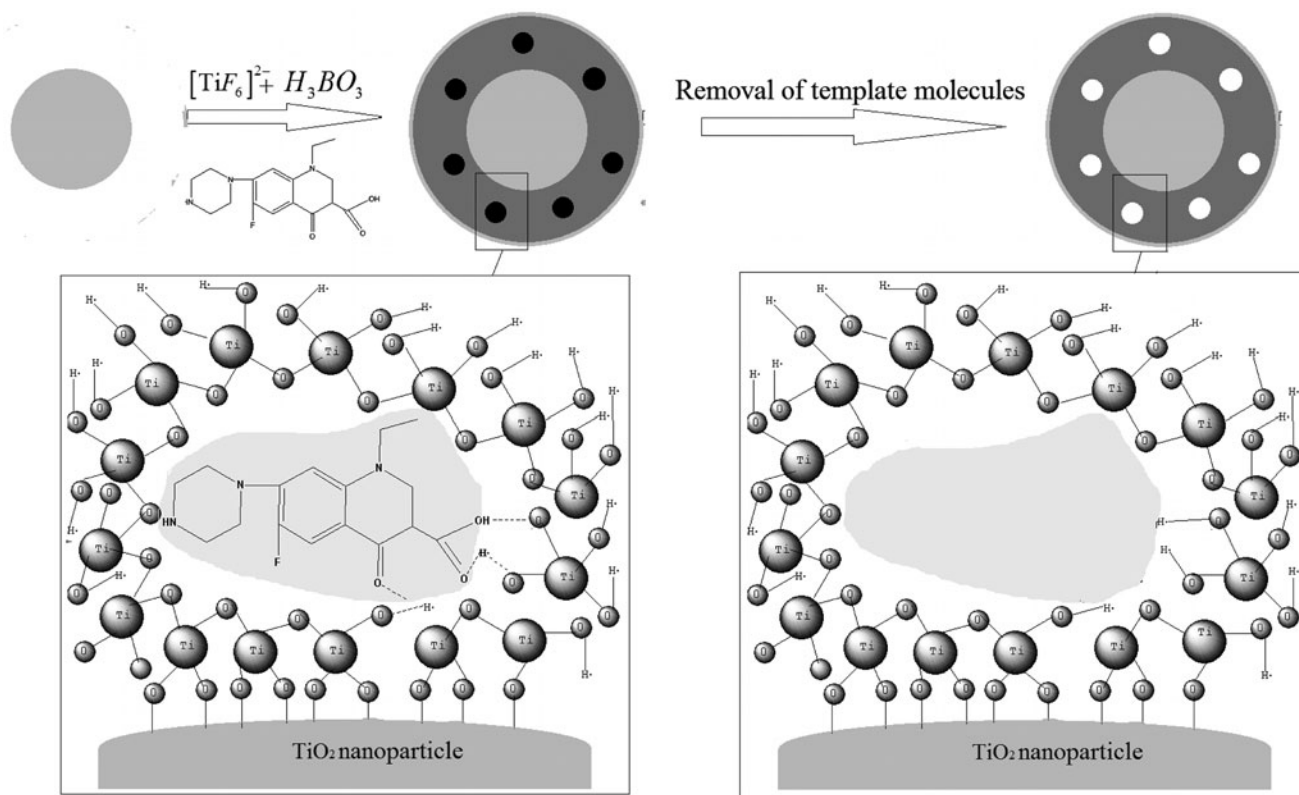


Fig. 1. Schematic procedure of the MIPs preparation.

The previous works have proved that this method could achieve the molecular imprinting on the surface of the supports namely the  $\text{TiO}_2$  nanoparticles [25]. However, the previous studies on the optimization of the MIPs preparation rarely considered the interaction of different factors. The significances of these factors could not be quantified simultaneously [18,19,26]. In this study, the effects of the concentrations of norfloxacin, ammonium hexafluorotitanate/boric acid, imprinting temperature, and imprinting time were comprehensively and simultaneously investigated based on the orthogonal experiments. As shown in Eqs. (2)–(4), when the fluorine in  $[\text{TiF}_{6-n}(\text{OH})_n]^{2-}$  was totally consumed, the theoretical reaction mole ratio of ammonium hexafluorotitanate to boric acid should be 2/3. To improve the utilization of ammonium hexafluorotitanate, the mole ratio of ammonium hexafluorotitanate to boric acid was set to 1/2. An  $L_9$  orthogonal array, which contained the four factors and three levels for each factor, was formed. The data were analyzed by SPSS 18.0 and the results were shown in Table 1. The mean values of removal efficiency under each factor would be calculated and the factor level that corresponded to the highest value for each factors was chosen as the optimal level.

The results indicated that the optimum concentrations of the norfloxacin and the ammonium hexafluorotitanate were  $200 \text{ mg L}^{-1}$  and  $0.02 \text{ mol L}^{-1}$ , respectively. The optimum imprinting temperature and time were  $30^\circ\text{C}$  and 2 h, respectively. The MIPs and NIPs used in the following experiments were prepared under this condition. The concentrations of ammonium hexafluorotitanate/boric acid seemed to be the most significant factor that affected the MIPs adsorption properties for norfloxacin in our experiments ( $p = 0.001$ ). The imprinting time was the second important factor ( $0.01 < p < 0.05$ ). The imprinting temperature and the concentrations of norfloxacin turned out to have only limited influence for the MIPs preparation ( $p > 0.05$ ).

### 3.2. Characterization of prepared samples

The morphology and particle size distributions of MIPs (before and after calcination) and P25 were shown in Fig. 2. The MIPs before and after calcination displayed the average sizes of approximately 37 and 43 nm, respectively, which were larger than the P25 with an average size of approximately 26 nm. The specific surface area of the MIPs, the NIPs, and P25

Table 1  
Effects of the preparation conditions on the MIPs adsorption performance (indicated by removal efficiency)

Factors	Factors level	Removal efficiency mean value	95% Confidence interval		<i>p</i>	Optimal level
			Lower limit	Higher limit		
Norfloxacin	100 mg L <sup>-1</sup>	0.56	0.65	0.48	0.67	200
	200 mg L <sup>-1</sup>	0.58	0.66	0.49		
	300 mg L <sup>-1</sup>	0.53	0.61	0.45		
Ammonium hexafluorotitanate/ boric acid	0.005/ 0.01 mol L <sup>-1</sup>	0.43	0.51	0.34	0.001	0.02/0.04
	0.01/ 0.02 mol L <sup>-1</sup>	0.57	0.65	0.49		
	0.02/ 0.04 mol L <sup>-1</sup>	0.67	0.75	0.59		
Reaction temperature	30 °C	0.60	0.68	0.51	0.419	30
	40 °C	0.55	0.63	0.47		
	50 °C	0.52	0.61	0.44		
Deposition time	0.5 h	0.56	0.64	0.48	0.011	2
	1 h	0.46	0.54	0.38		
	2 h	0.65	0.73	0.57		

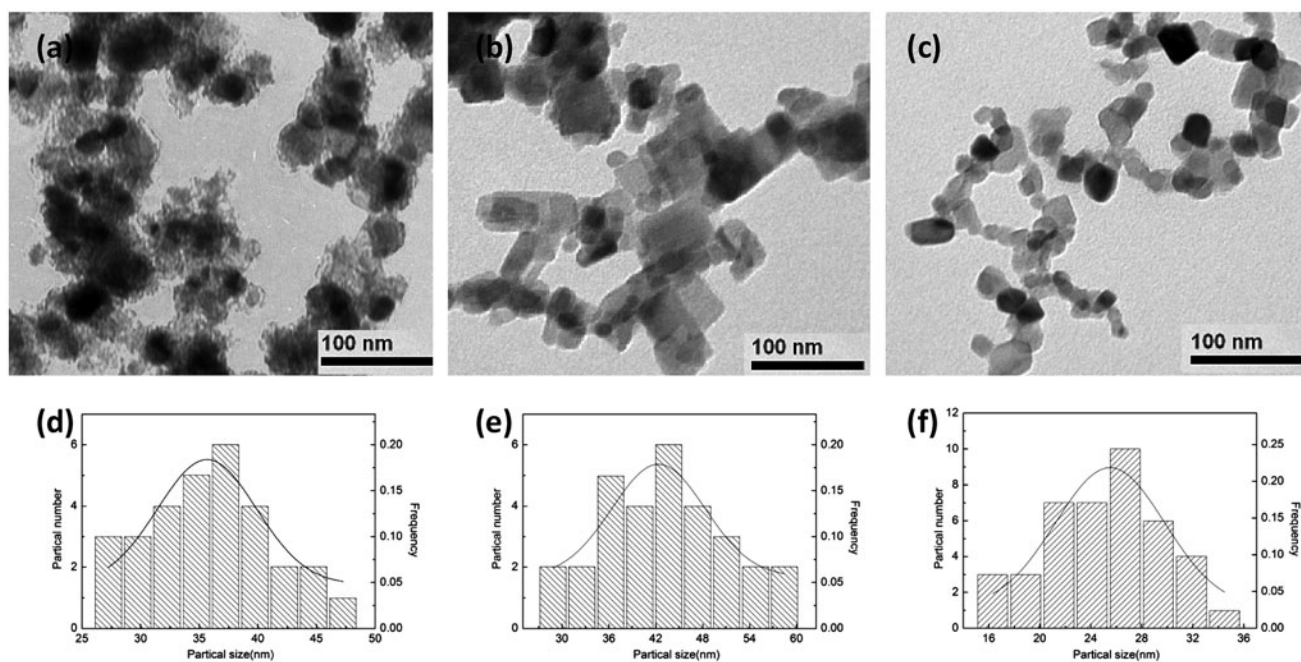


Fig. 2. The TEM micrographs of (a) the MIPs before calcination, (b) the MIPs after calcination, (c) P25 and the particle size distributions of, (d) the MIPs before calcination, (e) the MIPs after calcination, and (f) P25.

was found to be 63.2, 27.5, and 36.6 m<sup>2</sup> g<sup>-1</sup>, respectively. Furthermore, the total pore volume of the MIPs was 0.1 cm<sup>3</sup> g<sup>-1</sup>, which was 1.81 and 1.43 times more

than those of the NIPs and P25, respectively. The greater specific surface area and pore volume of the MIPs could enhance their adsorption performance.

Fig. 3 shows the XRD patterns obtained for the MIPs, the NIPs, and P25. All of the three adsorbents were contained anatase form, which implied by the peaks at the diffraction angle of about  $25^\circ$ . The existence anatase form indicated a good photocatalytic property of the adsorbents [27]. The XRD patterns proved that the crystal form was not changed during the preparation process. The MIPs and the NIPs should have the similar photocatalytic performance compared with P25. Hence, the MIPs would have favorable photocatalytic property as well as good adsorption ability.

### 3.3. Adsorption behavior of MIPs

#### 3.3.1. The optimal adsorbent dosage

Different dosages of the MIPs were employed to determine the optimal adsorbent dosage in order to remove norfloxacin from the aqueous solution efficiently and economically. According to the result, the adsorbent dosage had a great influence on the adsorption capacity of the MIPs. The removal efficiency of norfloxacin improved significantly with the increase in the dosage under  $1 \text{ g L}^{-1}$  and then the improvement remarkably slowed down with the further increase in the MIPs dosage. Comprehensively, considering the efficiency and economy,  $1 \text{ g L}^{-1}$  was chosen as the optimal adsorbent dosage.

#### 3.3.2. Adsorption kinetics

The kinetics for adsorption of norfloxacin onto the MIPs, the NIPs, and P25 were examined. The results correlated with the first- and second-order adsorption

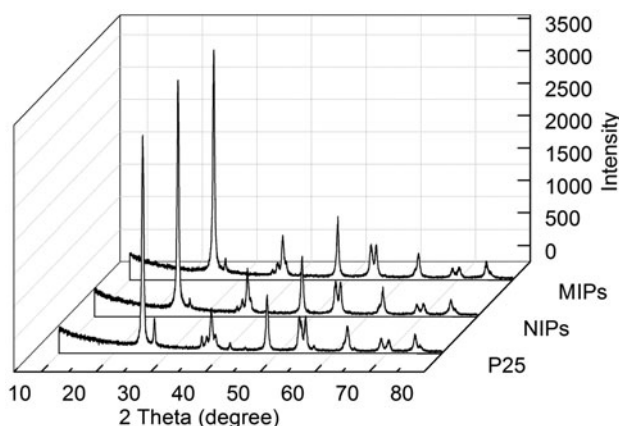


Fig. 3. XRD spectra of (a) the MIPs, (b) the NIPs, and (c) P25.

models were shown in Fig. 4 and the parameters were summarized in Table 2. The kinetic data of the MIPs correlated pseudo-second-order model better with the higher correlation coefficients ( $R^2 > 0.99$ ) and showed better agreements between  $q_{\text{exp}}$  and  $q_{\text{cal}}$  ( $\Delta p < 5\%$ ). The adsorption process for the NIPs and P25 was both fitted pseudo-second-order model and pseudo-first-order model well.

For all the adsorbents, norfloxacin adsorption reached equilibrium within 60 min, and no appreciable changes were noticed after that. The initial adsorption rate of the MIPs ( $0.491 \text{ g mg}^{-1} \text{ min}^{-1}$ ) was greater than that of the NIPs ( $0.259 \text{ g mg}^{-1} \text{ min}^{-1}$ ) and P25 ( $0.256 \text{ g mg}^{-1} \text{ min}^{-1}$ ). In the previous work, the norfloxacin was adsorbed by lotus stalk-based activated carbon, iron-doped activated alumina, hypercrosslinked resin, and aminated polystyrene resin [6,13]. The adsorption rate constant was  $2.2 \times 10^{-3}$ ,  $4.2 \times 10^{-5}$ ,  $7.4 \times 10^{-3}$ , and  $3.7 \times 10^{-2} \text{ g mg}^{-1} \text{ min}^{-1}$ , respectively, which were much lower than that of the MIPs. The higher adsorption rate of the MIPs could attributed to that the adsorption of norfloxacin onto the MIPs occurred mainly on the surface adsorption sites, while the adsorption sites of the other adsorbents mentioned above existed mainly in the internal pores and the adsorbed norfloxacin had the internal diffusion processes. Moreover, compared with the NIPs and P25, the MIPs had a higher initial adsorption rate and adsorption capacity for norfloxacin, indicating that the imprinting process could enhance the affinity for the norfloxacin molecule. Considering that the adsorption rate and the capacity were proportional to the number of active sites on the adsorbent [28], it

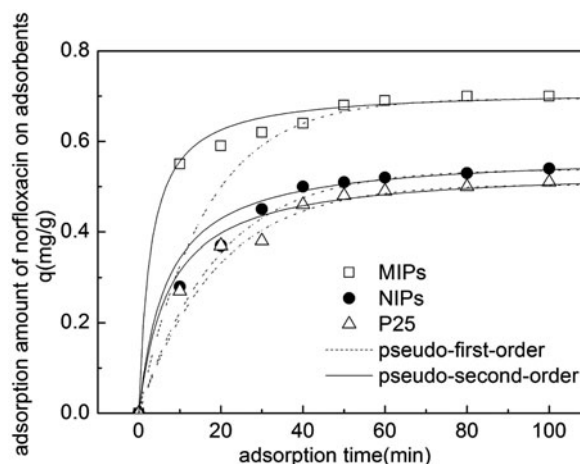


Fig. 4. Adsorption kinetics of the MIPs, the NIPs, and P25 for norfloxacin ( $c_1 = 1.0 \text{ mg L}^{-1}$ , adsorbent dosage =  $1.0 \text{ g L}^{-1}$ , pH 6.5,  $T = 25^\circ\text{C}$ ).

Table 2

Kinetic parameters of the pseudo-first- and second-order models for adsorption of norfloxacin on the MIPs, the NIPs, and P25

Adsorbent	Pseudo-first-order model <sup>a</sup>			Pseudo-second-order model <sup>b</sup>		
	$k_1$ (min <sup>-1</sup> )	$R^2$	$\Delta p$ (%) <sup>c</sup>	$k_2$ (g mg <sup>-1</sup> min <sup>-1</sup> )	$R^2$	$\Delta p$ (%)
MIPs	0.0632	0.946	15.43	0.4913	0.998	3.19
NIPs	0.0535	0.986	7.74	0.2590	0.990	10.14
P25	0.0534	0.987	8.98	0.2555	0.988	8.74

$$^a \ln(q_e - q) = \ln q_e - k_1 t.$$

$$^b \frac{t}{q} = \frac{1}{k_2 q_e^2} + \frac{1}{q_e} t.$$

$$^c \Delta p (\%) = 100 \sqrt{\frac{\sum \left[ \frac{(q_{\text{exp}} - q_{\text{cal}})^2}{q_{\text{exp}}} \right]}{N - 1}}.$$

where  $\Delta p$  (%) was the normalized standard deviation;  $q_{\text{exp}}$  and  $q_{\text{cal}}$  (mg g<sup>-1</sup>) were the experimental and model calculated norfloxacin sorption amounts;  $N$  was the number of measurements made.

could be inferred that the specific recognition sites on the surface of the MIPs were successfully created.

### 3.3.3. Adsorption isotherm

Adsorption isotherm experiments were performed to evaluate the adsorption capacity of the adsorbents. The data were fitted by Langmuir model and Freundlich model and related results were shown in Fig. 5 and Table 3.

It could be observed that the adsorption isotherms of the MIPs, the NIPs, and P25 correlated with Langmuir model better than Freundlich model ( $R^2 > 0.99$ ). Considering that the Langmuir model was derived based on the hypothesis of monolayer adsorption on specific homogenous sites [29], it could be inferred that the adsorption of norfloxacin on all the

three adsorbents occurred on their surface by monomolecular layer adsorption. The adsorption amount would increase with the increase in norfloxacin concentration and it would reach the maximum when the available sites were saturated with norfloxacin molecules. Moreover, the maximum adsorption capacity ( $q_m$ ) of the MIPs was 1.45 and 1.52 times higher than those of the NIPs and P25, respectively. In comparison with some adsorbents studied in the previous works [30,31], the MIPs had a greater adsorption capacity as well as the Langmuir constant ( $K_L$ ) for the norfloxacin, which indicated the increase in active adsorption sites and stronger adsorption affinity on the MIPs. As the MIPs, NIPs, and P25 were all constituted by the titanium–oxygen structures, the enhanced adsorption affinity should be mainly caused by the predetermined imprinted sites, which were called footprint cavity in the previous work [32]. Meanwhile, the increase in the specific surface area of the adsorbents after imprinting was greater than the increase in adsorption capacity and Langmuir constant for norfloxacin. It could be due to the inaccessibility of some imprinted sites ensconced inside the particles for norfloxacin. Besides, previous works have found that in non-covalent molecular imprinting, hydrophobic impact, H-bond, etc. could also have influence on the adsorption performance [13,33]. It could be inferred that the greater specific surface area and stronger intermolecular forces between the norfloxacin and MIPs enhanced the adsorption performance.

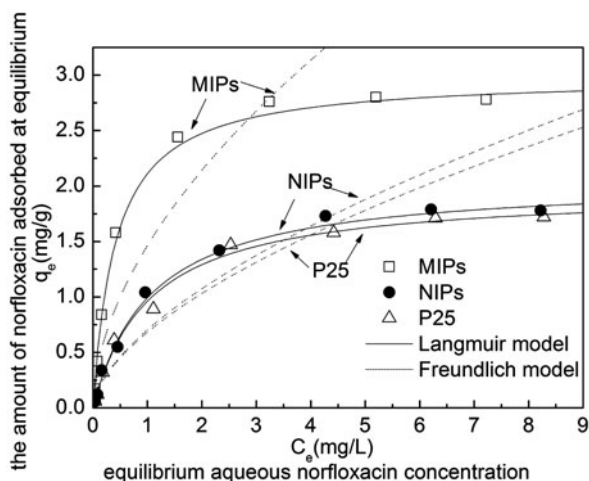


Fig. 5. Adsorption isotherms of the MIPs, the NIPs, and P25 for norfloxacin (adsorbent dosage = 1.0 g L<sup>-1</sup>, pH 6.5,  $T = 25^\circ\text{C}$ ,  $t = 4.0$  h).

### 3.3.4. Thermodynamic parameters

The effects of temperature on the adsorption were studied and the thermodynamic parameters of adsorption such as standard free energy change ( $\Delta G^0$ ), standard enthalpy change ( $\Delta H^0$ ), and standard entropy

Table 3

The Langmuir and Freundlich isotherm model parameters for adsorption of norfloxacin on the MIPs, the NIPs, and P25

Adsorbent	Langmuir model <sup>a</sup>			Freundlich model <sup>b</sup>		
	$q_m$ (mg/g)	$K_L$ (L/mg)	$R^2$	$K_F$ (mg/g(L/mg) <sup>1/n</sup> )	$1/n$	$R^2$
MIPs	2.99	2.402	0.999	1.46	0.550	0.943
NIPs	2.06	0.930	0.996	0.70	0.611	0.914
P25	1.96	0.961	0.997	0.68	0.597	0.942

$$c_e^{ac_{eq}} = c_e \cdot \frac{1}{q_m} + \frac{1}{K_L q_m}$$

<sup>b</sup> $\log q_e = \log K_F + \frac{1}{n} \log c_{eq}$ , where  $q_e$  (mg g<sup>-1</sup>) was the amount of norfloxacin adsorbed at equilibrium,  $q_m$  (mg g<sup>-1</sup>) was the maximum norfloxacin adsorption capacity.

Table 4

Recognition of different competitive molecules on the adsorbents

$K_d^a$	Norfloxacin	Ciprofloxacin	Carbamazepine	Phenol
MIPs	3.35	3.72	0.09	0.03
NIPs	1.17	1.16	0.08	0.02
P25	1.15	1.03	0.12	0.03

<sup>a</sup> $K_d = \frac{c_p}{c_e}$ , where  $K_d$  (L g<sup>-1</sup>) was the distribution coefficient,  $c_p$  (mg g<sup>-1</sup>) was the adsorption amount of norfloxacin on the adsorbents,  $c_e$  (mg L<sup>-1</sup>) was the amount of norfloxacin in aqueous solution at adsorption equilibrium.

change ( $\Delta S^0$ ) were calculated. The results were shown in Fig. 6. The standard free energy changes were all negative values, while the  $\Delta H^0$  and  $\Delta S^0$  values were all positive for all three adsorbents. The positive values of  $\Delta H^0$  indicated that the adsorption was an endothermic process. Previous works had found that higher temperature could have the negative [34], positive [13], and no significant [33] influences on adsorption process. The effect of temperature on the adsorption process depended on the positive or negative factors that dominated the adsorption process. For

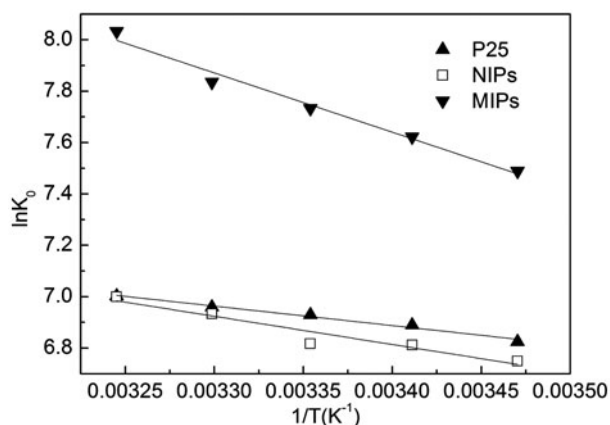


Fig. 6. Vant Hoff's plot for norfloxacin adsorption by the MIPs, the NIPs, and P25 ( $c_1 = 1.0$  mg L<sup>-1</sup>, adsorbent dosage = 1.0 g L<sup>-1</sup>, pH 6.5,  $t = 4.0$  h).

the MIPs, the NIPs, and P25, the increase in temperature could enhance the adsorption performance. The adsorption amounts of norfloxacin on MIPs at equilibrium increased about 15% when the reaction temperature was increased from 15 to 35°C. Possible explanation could be that the molecular motion would be more vigorous at higher temperature, and it could help more norfloxacin molecules overcome potential barriers at the aperture of the pores and reach the adsorption sites. This mechanism had also been described as gating effect in the previous work for the temperature effects on adsorption of krypton and xenon [35]. In addition, the pore diffusion process and the package density of adsorbate molecules in the micropores of adsorbents would be enhanced when the temperature increased. Yang et al. [13] have pointed out that the effect of micropore filling would be enhanced at higher temperature while H-bond formation and hydrophobic effect would be adverse. Hence, it could be inferred that for the non-covalent MIPs, micropore-filling effect had the greater contribution to adsorption than the intermolecular forces effect. Moreover, the negative values of  $\Delta G^0$  and positive value of  $\Delta S^0$  proved that the adsorption process was feasible and spontaneous at the range of 15–35°C.

#### 3.4. The selectivity of the adsorption by MIPs

The adsorption performance of the MIPs for ciprofloxacin, carbamazepine, and phenol was also tested to

investigate the adsorption selectivity of the MIPs. The results were shown in Fig. 7 and Table 4. As shown in Table 4, the MIPs had higher distribution coefficients for norfloxacin and ciprofloxacin compared with the NIPs and P25. The distribution coefficients for carbamazepine and phenol were low in all situations. In a word, the imprinting process could enhance the adsorption capacity for norfloxacin and ciprofloxacin but had no significant influence for carbamazepine and phenol. As norfloxacin and ciprofloxacin both owned hydroxyl, carboxyl, piperazine, fluorine, and similar molecular weight, it could be inferred that the molecular structures, functional groups, and molecular weight would be the main factors which influenced the adsorption selectivity. The previous work [36,37] using molecular imprinted polymers for the analysis of norfloxacin showed that the imprinted polymers had the favorable adsorption ability for both norfloxacin and ciprofloxacin. Analogous inference was made in the previous work using Cl-TiO<sub>2</sub> imprinted photocatalyst for the degradation of tetracycline [38]. The substances with the similar structures of the template molecule could also be effectively bound and removed on the molecular imprinted material. It could be concluded that the active adsorption sites created by molecular imprinting process provided extra and specific adsorption capacity for norfloxacin and its homologs with similar structures, functional groups, and molecular weight.

### 3.5. Regeneration characters

Considering that the MIPs should have good photocatalytic ability as evidenced by XRD analysis. Photodegradation was a moderate regeneration

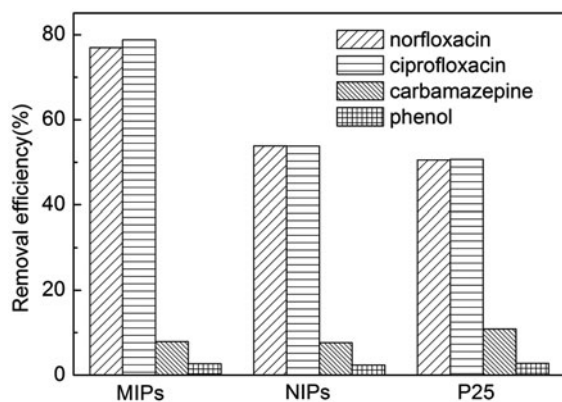


Fig. 7. Removal efficiency of norfloxacin, ciprofloxacin, carbamazepine, and phenol on the MIPs, the NIPs, and P25 ( $c_1 = 1.0 \text{ mg L}^{-1}$ , adsorbent dosage =  $1.0 \text{ g L}^{-1}$ , pH 6.5,  $T = 25^\circ\text{C}$ ,  $t = 4.0 \text{ h}$ ).

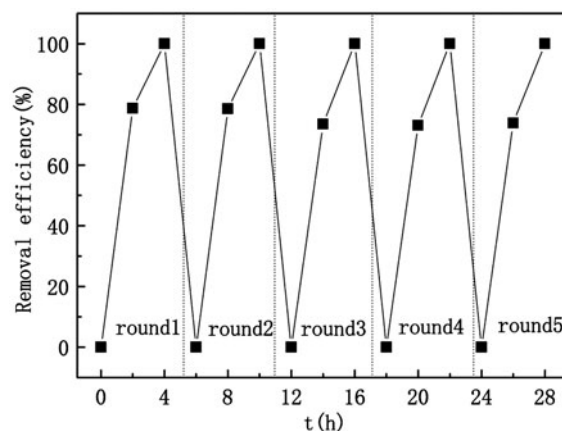


Fig. 8. Removal efficiency of norfloxacin during reuse cycles ( $c_1 = 1.0 \text{ mg L}^{-1}$ , adsorbent dosage =  $1.0 \text{ g L}^{-1}$ , pH 6.5,  $T = 25^\circ\text{C}$ ,  $t = 4.0 \text{ h}$ ).

method which could effectively degrade the norfloxacin adsorbed on the MIPs. Hence, UV irradiation was chosen as the regeneration method for the MIPs. The adsorption experiments were performed to determine whether the MIPs could maintain the adsorption performance within several reuse cycles. As shown in Fig. 8, the results proved that the removal efficiency of norfloxacin by the MIPs hardly decreased within five reuse cycles. The demonstrated reusability of the MIPs over several cycles showed an advantage in practical use. Moreover, the molecular imprinted adsorbents were mainly regenerated using deionized water, acid, lye, and organic solvent in previous works [17,18,26]. Compared with these regeneration methods, UV irradiation regeneration caused less waste and was more environmental friendly. In addition, the norfloxacin could be degraded during the regeneration process. The study about the degradation character of norfloxacin on the MIPs was in progress.

## 4. Conclusions

The novel MIPs were prepared by a surface molecular imprinting technique with P25 nanoparticles as the support and norfloxacin as the template. The adsorption of norfloxacin on the MIPs, the NIPs, and P25 was endothermic process and it followed the second-order adsorption model and Langmuir model. The MIPs prepared under optimized condition indicated higher adsorption rate and capacity toward norfloxacin compared with the NIPs and P25 owing to the imprinted sites and higher surface area. Molecular structures and properties played important roles in selectivity of the adsorption by MIPs. Moreover, the

MIPs could be regenerated under UV irradiation at least five times without reducing the removal efficiency significantly, which was more economical, efficient, and environmental-friendly than the traditional regeneration methods. The results confirmed that MIPs had been successfully prepared and they would have a potential application in the removal of trace norfloxacin from the aquatic environment.

### Acknowledgments

This work was financially supported by Zhejiang Provincial Natural Science Foundation of China (No. LQ12B07002), the National Natural Science Foundation of China (No. 51108406) and National Science and Technology Major Project for Water Pollution Control and Treatment (No. 2012ZX07403-003).

### References

- [1] R. Hirsch, T. Ternes, K. Haberer, K.L. Kratz, Occurrence of antibiotics in the aquatic environment, *Sci. Total Environ.* 225 (1999) 109–118.
- [2] M.M. Haque, M. Muneer, Photodegradation of norfloxacin in aqueous suspensions of titanium dioxide, *J. Hazard. Mater.* 145 (2007) 51–57.
- [3] E.M. Golet, A.C. Alder, W. Giger, Environmental exposure and risk assessment of fluoroquinolone antibacterial agents in wastewater and river water of the Glatt Valley Watershed, Switzerland, *Environ. Sci. Technol.* 36 (2002) 3645–3651.
- [4] T. An, H. Yang, W. Song, G. Li, H. Luo, W.J. Cooper, Mechanistic considerations for the advanced oxidation treatment of fluoroquinolone pharmaceutical compounds using TiO<sub>2</sub> heterogeneous catalysis, *J. Phys. Chem. A* 114 (2010) 2569–2575.
- [5] T.A. Ternes, A. Joss, H. Siegrist, Peer reviewed: Scrutinizing pharmaceuticals and personal care products in wastewater treatment, *Environ. Sci. Technol.* 38 (2004) 392A–399A.
- [6] W. Liu, J. Zhang, C. Zhang, L. Ren, Sorption of norfloxacin by lotus stalk-based activated carbon and iron-doped activated alumina: Mechanisms, isotherms and kinetics, *Chem. Eng. J.* 171 (2011) 431–438.
- [7] S. Zorita, L. Mártensson, L. Mathiasson, Occurrence and removal of pharmaceuticals in a municipal sewage treatment system in the south of Sweden, *Sci. Total Environ.* 407 (2009) 2760–2770.
- [8] M. Córdoba-Díaz, M. Córdoba-Borrego, D. Córdoba-Díaz, Modification of fluorescent properties of norfloxacin in the presence of certain antacids, *J. Pharm. Biomed. Anal.* 18 (1998) 565–571.
- [9] D.W. Kolpin, E.T. Furlong, M.T. Meyer, E.M. Thurman, S.D. Zaugg, L.B. Barber, H.T. Buxton, Pharmaceuticals, hormones, and other organic wastewater Contaminants in U.S. streams, 1999–2000: A national reconnaissance, *Environ. Sci. Technol.* 36 (2002) 1202–1211.
- [10] C.L. Amorim, A.S. Maia, R.B.R. Mesquita, A.O.S.S. Rangel, M.C.M. van Loosdrecht, M.E. Tiritan, P.M.L. Castro, Performance of aerobic granular sludge in a sequencing batch bioreactor exposed to ofloxacin, norfloxacin and ciprofloxacin, *Water Res.* 50 (2014) 101–113.
- [11] W. Li, C. Guo, B. Su, J. Xu, Photodegradation of four fluoroquinolone compounds by titanium dioxide under simulated solar light irradiation, *J. Chem. Technol. Biotechnol.* 87 (2012) 643–650.
- [12] J. Rivas, Á. Encinas, F. Beltrán, N. Graham, Application of advanced oxidation processes to doxycycline and norfloxacin removal from water, *J. Environ. Sci. Health, A* 46 (2011) 944–951.
- [13] W. Yang, Y. Lu, F. Zheng, X. Xue, N. Li, D. Liu, Adsorption behavior and mechanisms of norfloxacin onto porous resins and carbon nanotube, *Chem. Eng. J.* 179 (2012) 112–118.
- [14] A. Beltran, F. Borrull, R.M. Marcé, P.A.G. Cormack, Molecularly-imprinted polymers: Useful sorbents for selective extractions, *TrAC, Trends Anal. Chem.* 29 (2010) 1363–1375.
- [15] E. Rodríguez, F. Navarro-Villoslada, E. Benito-Peña, M.D. Marazuela, M.C. Moreno-Bondi, Multiresidue determination of ultratrace levels of fluoroquinolone antimicrobials in drinking and aquaculture water samples by automated online molecularly imprinted solid phase extraction and liquid chromatography, *Anal. Chem.* 83 (2011) 2046–2055.
- [16] E. Benito-Peña, S. Martins, G. Orellana, M.C. Moreno-Bondi, Water-compatible molecularly imprinted polymer for the selective recognition of fluoroquinolone antibiotics in biological samples, *Anal. Bioanal. Chem.* 393 (2009) 235–245.
- [17] B. Schweiger, L. Bahnweg, B. Palm, U. Steinfeld, Development of molecular imprinted polymers (MIPs) for the selective removal of carbamazepine from aqueous solution, *Proc. World Acad. Sci. Eng. Technol.* 54 (2009) 661–666.
- [18] Q. Yu, S. Deng, G. Yu, Selective removal of perfluorooctane sulfonate from aqueous solution using chitosan-based molecularly imprinted polymer adsorbents, *Water Res.* 42 (2008) 3089–3097.
- [19] L. Önnby, V. Pakade, B. Mattiasson, H. Kirsebom, Polymer composite adsorbents using particles of molecularly imprinted polymers or aluminium oxide nanoparticles for treatment of arsenic contaminated waters, *Water Res.* 46 (2012) 4111–4120.
- [20] Z. Zhongbo, J. Hu, Selective removal of estrogenic compounds by molecular imprinted polymer (MIP), *Water Res.* 42 (2008) 4101–4108.
- [21] Z. Zhang, J. Hu, Effect of environmental factors on estrogenic compounds adsorption by MIP, *Water Air Soil Pollut.* 210 (2010) 255–264.
- [22] W. Xing, L. Ni, X. Liu, Y. Luo, Z. Lu, Y. Yan, P. Huo, Synthesis of thermal-responsive photocatalysts by surface molecular imprinting for selective degradation of tetracycline, *RSC Adv.* 3 (2013) 26334–26342.
- [23] Y. Hsiao, T. Wu, Y. Wang, C. Hu, C. Huang, Evaluating the sensitizing effect on the photocatalytic decoloration of dyes using anatase-TiO<sub>2</sub>, *Appl. Catal., B* 148–149 (2014) 250–257.
- [24] X. Luo, F. Deng, L. Min, S. Luo, B. Guo, G. Zeng, C. Au, Facile one-step synthesis of inorganic-framework molecularly imprinted TiO<sub>2</sub>/WO<sub>3</sub> nanocomposite and its molecular cognitive photocatalytic degradation of

- target contaminant, *Environ. Sci. Technol.* 47 (2013) 7404–7412.
- [25] X. Shen, L. Zhu, H. Yu, H. Tang, S. Liu, W. Li, Selective photocatalysis on molecular imprinted TiO<sub>2</sub> thin films prepared via an improved liquid phase deposition method, *New J. Chem.* 33 (2009) 1673–1679.
- [26] Y. Ren, W. Ma, J. Ma, Q. Wen, J. Wang, F. Zhao, Synthesis and properties of bisphenol a molecular imprinted particle for selective recognition of BPA from water, *J. Colloid Interface Sci.* 367 (2012) 355–361.
- [27] D.S. Bhatkhande, V.G. Pangarkar, A. Beenackers, Photocatalytic degradation for environmental applications—A review, *J. Chem. Technol. Biotechnol.* 77 (2002) 102–116.
- [28] Y.S. Ho, J. Ng, G. McKay, Kinetics of pollutant sorption by biosorbents: Review, *Sep. Purif. Rev.* 29 (2000) 189–232.
- [29] B. Sellergren, Imprinted chiral stationary phases in high-performance liquid chromatography, *J. Chromatogr. A* 906 (2001) 227–252.
- [30] J. Zhang, Y. Dong, Effect of low-molecular-weight organic acids on the adsorption of norfloxacin in typical variable charge soils of China, *J. Hazard. Mater.* 151 (2008) 833–839.
- [31] A.C. Hari, R.A. Paruchuri, D.A. Sabatini, T. Kibbey, Effects of pH and cationic and nonionic surfactants on the adsorption of pharmaceuticals to a natural aquifer material, *Environ. Sci. Technol.* 39 (2005) 2592–2598.
- [32] G. Wulff, Enzyme-like catalysis by molecularly imprinted polymers, *Chem. Rev.* 102 (2002) 1–28.
- [33] A.S. Mestre, J. Pires, J.M.F. Nogueira, A.P. Carvalho, Activated carbons for the adsorption of ibuprofen, *Carbon* 45 (2007) 1979–1988.
- [34] E.M. Cuerda-Correa, J.R. Domínguez-Vargas, F.J. Olivares-Marín, J. de Heredia, On the use of carbon blacks as potential low-cost adsorbents for the removal of non-steroidal anti-inflammatory drugs from river water, *J. Hazard. Mater.* 177 (2010) 1046–1053.
- [35] C.A. Fernandez, J. Liu, P.K. Thallapally, D.M. Strachan, Switching Kr/Xe selectivity with temperature in a metal–organic framework, *J. Am. Chem. Soc.* 134 (2012) 9046–9049.
- [36] B. Zhang, J. Zhao, B. Sha, M. Xian, Selective solid-phase extraction using molecularly imprinted polymers for the analysis of norfloxacin in fish, *Anal. Methods* 4 (2012) 3187–3192.
- [37] Y. Lv, Y. Ma, X. Zhao, C. Jia, H. Sun, Grafting of norfloxacin imprinted polymeric membranes on silica surface for the selective solid-phase extraction of fluoroquinolones in fish samples, *Talanta* 89 (2012) 270–275.
- [38] X. Liu, P. Lv, G. Yao, C. Ma, P. Huo, Y. Yan, Microwave-assisted synthesis of selective degradation photocatalyst by surface molecular imprinting method for the degradation of tetracycline onto CITiO<sub>2</sub>, *Chem. Eng. J.* 217 (2013) 398–406.